# Production and Effects of Low-Energy Electrons in Helium*

ROBERT H. McFARLAND
*Lawrence Radiation Laboratory, University of California, Livermore, California*
(Received 13 May 1964)

Three low-energy electron guns have been constructed and tested, using the elastic scattering resonance in helium to determine the energy resolution of the electron beam. Additional threshold excitation measurements have been made in an attempt to produce, in one laboratory, a comprehensive study involving the effectiveness of microampere-level, low-energy beams for producing metastable atoms and optically observable allowed transitions. The resulting data are presented. In addition, a second elastic resonance in helium has been observed, and the two resonances have been determined to be at 19.52±0.1 and 20.30±0.1 V.

## INTRODUCTION

RECENTLY renewed interest in atomic phenomena has led to enlarged research activity in studies involving threshold excitation[1,2] and polarization[3] in helium.

Other experimentalists[4–6] have investigated elastic scattering, with the observation of interesting new elastic-scattering resonances. Theories[6–13] have been proposed to explain these observations.

The task of the theorist, unfortunately, has been complicated in this effort by the reticence of the experimentalist in the interpretation of his results. The work to be described here was undertaken in an attempt to perform—in one laboratory, under comparable conditions—a sufficient number of experiments using suppressed-current measuring techniques, metastable-produced secondary measurements, and spectrographic techniques to clarify some of the present misunderstandings. Primarily, these have involved the role and efficacy of the electron gun, the energy dependency of excitation curves, the threshold value, and the interpretation of composite intensities involving more than one cross section.

## APPARATUS

As it was desirable to make spectroscopic measurements with pressures and beam currents ranging from $10^{-1}$ to $10^{1}$ $\mu$ and $\mu$A, respectively, it was virtually a necessity that the electron gun selected for this work should be aperture-limited and focused, as opposed to the preferable (where applicable) low-energy-spread electrostatic-focusing systems developed by Marmet and Kerwin.[14] Figure 1 depicts three different gun geometries which were used in the preliminary phases of this experiment, along with a retarding potential evaluation taken by applying a retarding potential $V_R$ to an accelerating electrode, and keeping all other conditions constant including the collector-cup potentials. Gun 1 was a scaled down version of a double-immersion-lens type of gun used by Simpson[15] for high-energy electrons. Gun 2 has been described previously.[2] Gun 3 used the principle developed by Fox and co-workers,[16] and was designed to the approximate specifications given by Schulz and Fox.[17] For reasons presented later, gun 2 was mated to two different interaction chambers shown in

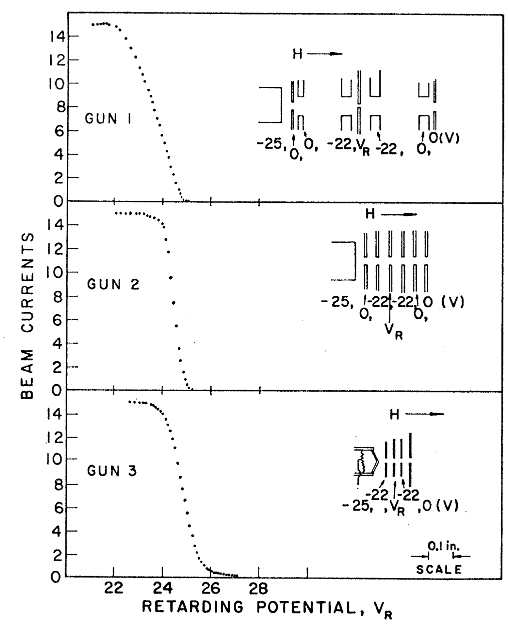


FIG. 1. Electron-gun geometries and retarding-potential measurements for 25-V electron beams. The scale shown applies to all three guns.

* Work done under the auspices of the U. S. Atomic Energy Commission.

[1] C. Smit, H. G. M. Heideman, and J. S. Smit, Physica **29**, 245 (1963).
[2] G. S. Higginson and L. W. Kerr, Proc. Phys. Soc. (London) **77**, 866 (1961).
[3] R. H. McFarland, Phys. Rev. **133**, A986 (1964).
[4] G. J. Schulz, Phys. Rev. Letters **10**, 104 (1963).
[5] R. J. Fleming and G. S. Higginson, Proc. Phys. Soc. (London) **81**, 974 (1963).
[6] J. A. Simpson and U. Fano, Phys. Rev. Letters **11**, 158 (1963).
[7] E. P. Wigner, Phys. Rev. **73**, 1002 (1948).
[8] G. H. Wannier, Phys. Rev. **100**, 1180 (1956).
[9] S. Geltman, Phys. Rev. **112**, 176 (1958).
[10] H. S. W. Massey and B. L. Moiseiwitsch, Proc. Roy. Soc. (London) **A227**, 38 (1954).
[11] I. C. Percival and M. J. Seaton, Phil. Trans. Roy. Soc. (London) **A251**, 113 (1958).
[12] E. Gerjuoy, J. Appl. Phys. **30**, 28 (1959).
[13] P. G. Burke and H. M. Schey, Phys. Rev. **126**, 147 (1962).
[14] P. Marmet and L. Kerwin, Can. J. Phys. **38**, 787 (1960).
[15] J. A. Simpson, Rev. Sci. Instr. **32**, 1283 (1961).
[16] R. E. Fox, W. M. Hickman, D. J. Grove, and T. Kjeldaas, Rev. Sci. Instr. **26**, 1101 (1955).
[17] G. J. Schulz and R. E. Fox, Phys. Rev. **106**, 1179 (1957).

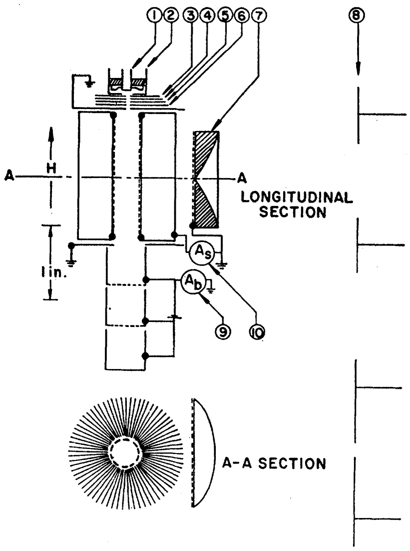


FIG. 2. Electron gun and interaction chamber used for optical intensity measurements and elastic scattering. Legend: 1. Cathode, $-V_c$; 2. First accelerating electrode, $-V_c+5$; 3. Second accelerating electrode, $-V_c+15$; 4. Third accelerating electrode, ground; 5. Fourth accelerating electrode, $-V_c+5+\sqcup\sqcap$; 6. Fifth accelerating voltage, ground; 7. Cylindrical quartz lens; 8. B. and L. 500-mm monochrometer; 9. Beam current electrometer; 10. Scattered current electrometer.

Figs. 2 and 3. Both chambers were capable of measuring the elastic-scattering cross section by observing both the scattered and beam currents, and of retarding potential measurements at the gun and at the beam collector. The interaction chamber of Fig. 2 was designed to minimize the effects of elastically scattered electrons and scattered light. This chamber, as well as the accompanying light measuring apparatus, has been described previously.[2] Figure 3 shows a chamber adapted from a similar one used by Schulz and Fox[17] for measurement of the intensity of helium metastables.

All parts of the guns and chambers were gold-plated nonmagnetic stainless steel except for the fins in Fig. 2. These were platinum-black-coated (electrolytically deposited) subsequent to gold plating. Dimensions are obtainable from the figures. The limiting apertures in the guns, both of the second type, were 0.030 in. in diameter. Spacing between accelerating electrodes was 0.050 in. The cathodes were indirectly heated, and constructed of barium impregnated tungsten. The gold grids were of 40 lines-per-inch spacing and 87% transmission.

Vacuum was provided in the stainless system by Vacsorb and Vacion pumps, with liquid-nitrogen-cooled Vacsorb pumps allowed to operate during the experiment. Base pressure for the baked system was of the order of $10^{-9}$ and $10^{-7}$ Torr or less with the cathode hot. Further purification of the inert gases was provided by a hot titanium filament immersed in the gas. Pressures were determined by use of ionization gages calibrated against McLeod gages for the gas used.

Measurement of radiation emitted by the electron bombardment of gases was accomplished by the use of a Bausch and Lomb 500-mm monochromator with detection by an E.M.I. 6256-S photomultiplier tube. Conventional phase detection at 100 cycles/sec was utilized to minimize noise.

As in previous work,[17,18,19] metastables were detected in the chamber of Fig. 3 after their having drifted to a gold-plated electrode. By virtue of their excitation energy, metastables caused electrons to be emitted from the surface in direct relationship to the metastable flux. Because of previous recognition[2] that elastically scattered electrons contribute to the production of excited atoms, a change in grid biasing was considered necessary. Schultz provided a positive 15-V bias on the outer grid, for the purpose of collecting the electrons ejected by the metastable atoms incident on the cylindrical surface. This has a function of accelerating the elastically scattered component of the beam current to energies as much as 15 V above that within the beam. This is observable in terms of early collections of electrons and, later, ions. It also provides potential leakage through the inner grid, which leads to a lesser knowledge of the beam energy.

After a series of measurements, it was determined that with the outer grid at a negative 3 V, and the outer cylinder at either the cathode potential or a constant negative 18 V, the undesirable effects of a positive potential on the outer grid could be eliminated.

## RESULTS

Figure 4 is a composite of a series of measurements using the chamber of Fig. 2. The first of these simultaneously measured the scattered and beam currents and the threshold intensity of helium lines 4922 and 4388 Å, in $10^{-2}$ Torr of helium as a function of applied accelerating voltage (measured with a Fluke 801 HR differential voltmeter). The excitation-efficiency curves, intensity per unit current versus accelerating voltage for these two lines, chosen because they are relatively

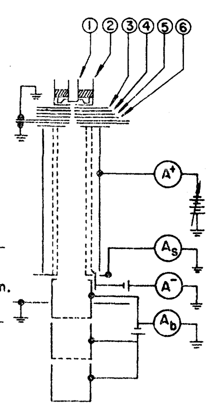


FIG. 3. Electron gun and interaction chamber used for metastable-atom-production measurements and elastic scattering. Legend: 1. Cathode, $-V_c$; 2. First accelerating electrode, $-V_c+3$; 3. Second accelerating electrode, $-V_c+15$; 4. Third accelerating electrode, ground; 5. Fourth accelerating electrode, $-V_c+(5\rightarrow 10)$; 6. Fifth accelerating electrode, ground; $A^+$: positive-ion and metastable atom electrometer; $A_s$: scattered electron electrometer; $A^-$: electron-monitoring electrometer; $A_b$: beam current electrometer.

[18] H. Maier-Leibnitz, Z. Physik 9, 499 (1936).
[19] R. Dorrestein, Physica 9, 447 (1942).

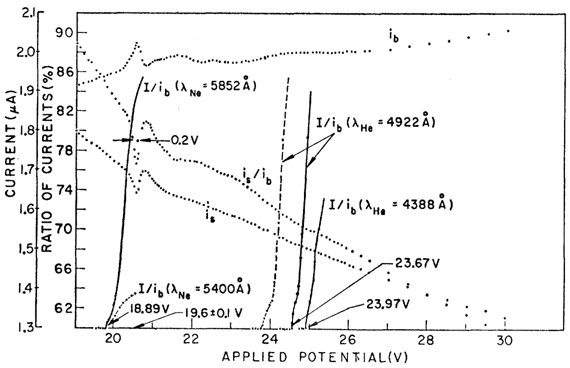


FIG. 4. Threshold measurements and voltage calibrations of the elastic-scattering resonance in terms of optical measurements. The scale for the relative excitation efficiency curves is not shown, as the purpose of the curves is only to indicate their threshold potentials. It is understood, however, to be linear, and extends from a zero initial value.

pressure insensitive, are the solid line curves, while the actual data points are plotted for the beam and scattered currents and their ratio.

Also plotted in Fig. 4 are the results of a second series of measurements in which 10% neon was added to the helium. No shift in the elastic resonance with respect to the applied voltage was observed.

The threshold excitation efficiency of neon lines 5852 and 5400 Å are shown, along with dashed curve corresponding to helium 4922 Å. The displacement of the dashed from the solid curve representing this helium line is due to the neutralizing effects of the neon ion produced in the helium neon mixture at 21.47 V on surface and space charges (22.42 V applied potential).

Figure 5 presents measurements of the scattered and beam currents and $i^+$, the current from the outer cylinder, made with the interaction chamber of Fig. 3. Also shown in dashed curves are semiquantitatively derived excitation efficiencies of excitation levels which contribute to $i^+$. An enlarged section of the threshold values of $i^+$, and the energy distribution of the electron beam as is inferred by the elastic scattering measurement, are shown in Fig. 6.

While no one has successfully separated the effects responsible for the production of the $i^+$ curve, some help in its interpretation may be obtained from examining the excitation curves of comparable transitions in optical spectra. Such curves obtained by use of the interaction chamber shown in Fig. 2 are to be seen in Fig. 7.

## DISCUSSION OF RESULTS

Probably the two most important features presented in Figs. 4 and 5 involves the suggestion in Fig. 5 of a heretofore unreported elastic resonance at 20.30 eV, and the possibility of using nearby inelastic-collision events for energy calibration of both elastic resonances. Interpretation of these results with regard to energy is dependent upon an understanding of low-energy electron guns.

Smit and co-workers[1] have discussed the effects of space charging, contact potentials, cathode temperature, and other electron-energy spreading effects in excellent detail. Surface charging can also be effective in shifting onset potentials. Ionization of the gas or impurities within the gas tend to neutralize this effect. The above workers[1] estimate a lower limit on the energy resolution from theory of 0.2 to 0.3 V, which they appear to have approached in their experiments.

A number of workers[15,16,17] have used a retarding-potential-difference principle (R.P.D.) in an attempt to improve the energy resolution of an electron beam, but the problem of energy spread still exists at low energies. Understanding of the partial failure of this system to "sharply" cut off the low energy electrons can be best understood in terms of work by Glaser.[20] One can approximate the potential difference $\Delta V$ between the axis and a point at a radial distance $r$ in the plane of an aperture of radius $R$, between two fields of intensity $\epsilon_1$ and $\epsilon_2$, as

$$\Delta V = 2(\pi R)^{-1}(\epsilon_2 - \epsilon_1)r^2.$$

For a gun of type 1 with an $R$ of 0.0075 in. and the spacing between electrodes 0.036 in., $\Delta V$ is proportional to $r^2$ and varies between 0 and 0.8 V for values of $\epsilon$ which provide maximum focusing of 25 eV.

Thus, in such a retarding potential analysis as that above, a spread of energies exists in the electrons which penetrate the aperture dependent upon the $r$ value to which they are focused. This spread can be in addition

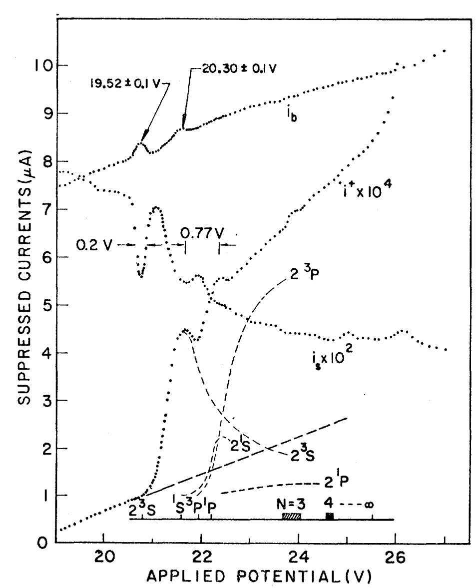


FIG. 5. Threshold measurements and voltage calibrations of the elastic-scattering resonances in terms of the production of metastables. The dashed $2\,^3P$, $2\,^1S$, $2\,^3S$, and $2\,^1P$ are relative-efficiency excitation curves normalized to the $i^+$ curve by assuming that its initial abrupt increase is due to the excitation of the $2\,^3S$ metastable level.

[20] A. Glaser and W. Henneberg, Z. Tech. Physik 17, 222 (1935).

to a second comparable one resulting from the final acceleration of the electron.

A second fault lies in the fact that the R. P. D. method has no effect on the radial motion of the electron. Heil[21] has attempted to eliminate these two effects by careful focusing, and by using 200-line-per-centimeter grids as multiple apertures.

A third fault less readily overcome, as seen in Fig. 1, results from the relatively small $\Delta i/\Delta V$. To the extent that the results are statistical, the errors will be relatively large, inasmuch as the difference in the two signals will always be small compared to the sums. Gun 2, although capable of improvement, exhibited the more desirable characteristics, and was chosen for the remaining measurements. Currents of a few microamperes were available at 2 V. Energy spread utilizing the elastic-scattering cross section was less than 0.25 V at 25 V; and with a 15-G magnetic field, focus into the collector was better than 98%.

Experimentally, with the two guns using indirectly heated cathodes, it has been possible to resolve the elastic resonance in helium with both sets of $i_b$ and $i_s$ and $i_s/i_b$ in a retarding-potential-difference experiment. For the same measurements, the scatter in $\Delta i_s$ and $\Delta i_b$ was too great to make them useful. For this reason, all of the present measurements were limited to direct measurements.

One can reasonably assume from the appearance of the elastic scattering resonance in Figs. 4 and 5 that the actual energy distribution of the electron beam is reasonably Gaussian. This distribution is effective for the production of metastables. As has been inferred previously,[2] the optical measurements utilize only a small portion of the electron beam, and result from both optical and electrical focusing to give maximal in-

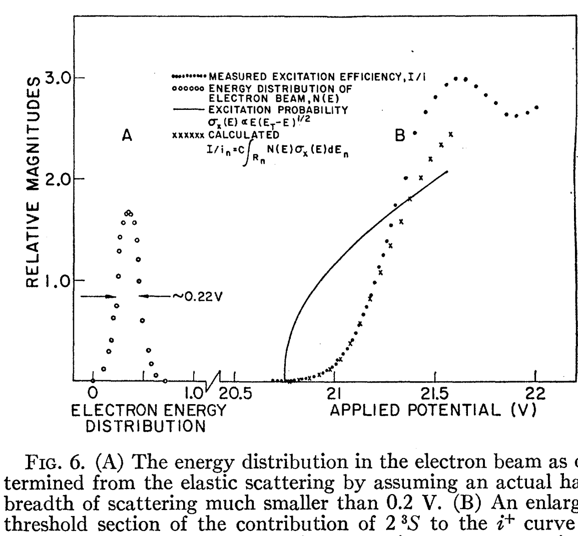


FIG. 6. (A) The energy distribution in the electron beam as determined from the elastic scattering by assuming an actual half-breadth of scattering much smaller than 0.2 V. (B) An enlarged threshold section of the contribution of $2\,^3S$ to the $i^+$ curve of Fig. 5. Also shown is an assumed cross-section curve proportional to the excess energy of the electron, and crosses corresponding to the calculated excitation per unit current.

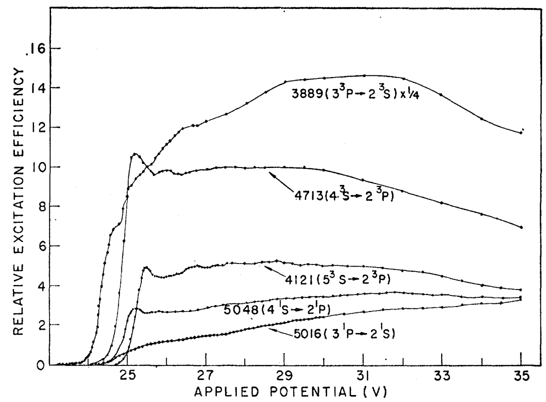


FIG. 7. Relative excitation per unit current curves versus applied-beam acceleration potential for selected optical transitions. The pressure was $2.5\times10^{-3}$ Torr, and the current was of the order of $1\times10^{-6}$ A.

tensity. It appears then, that over a few volts' range in applied potential, the useful energy resolution for optical measurements may be less than 0.1 V. This is demonstrated in terms of the threshold excitation curves of Fig. 4. It is unfortunate in these measurements, that the effective optical and electron beam energy resolutions are different for the two types of scattering being observed. The determination of $19.6\pm0.1$ eV as the energy of the elastic-scattering resonance was with the assumption that the effective electron beam for optical excitation be narrow and coincide with the center of the distribution effective for the elastic-scattering measurement. This obviously may result in error.

The measurements presented in Fig. 5 were made in an attempt to utilize the same effective energy resolution for both the calibration measurement and the scattering resonance. Further, the calibration utilizing the threshold of the metastable levels provided for an energy still closer to that of the resonance.

The energy calibration in Fig. 5 is relatively easy, inasmuch as the threshold for $I/i$ for the production of helium $2\,^3S_1$ corresponds directly to the threshold for the production of the elastic-scattering resonance. Figure 6 shows to some extent how this observed excitation efficiency curve $I/i$, represented by $i^+$, is produced. Probably never before has it been possible in a single experiment to measure an excitation function, and at the same time have available information concerning the energy distribution of the electron beam. This distribution, as derived with minimum assumptions from the elastic-scattering data, is shown at the left of Fig. 6. To the right, one can observe the measured excitation efficiency curve, an assumed excitation probability or cross section curve for excitation proportional to $E(E-E_T)^{1/2}$, and an excitation efficiency curve calculated from

$$I/i_N = C\int_{R_N} N(E)\sigma_X(E)dE_N.$$

[21] H. Heil, Bull. Am. Phys. Soc. 7, 488 (1962).

The integral over $R_N$ indicates a calculation for each energy setting from threshold energy $E_T$, to the extent of overlap of the electron beam distribution function of the cross section function $\sigma_X(E)$. The constant $C$ corrects for path length and pressure.

$N(E)$ is the electron energy distribution function. $\sigma_X(E)$, dependent over this small energy range on the square root of the excess energy of the electron $(E-E_T)^{1/2}$, has been adequately described by Wigner,[7] Wannier,[8] and Geltman.[9] The closeness of fit of the experimental to the calculated values, even for the limited range, seems satisfying proof of the square-root law. Also demonstrated is the fallacy of a rather common procedure of extrapolation of the straight line portion of the $I/i$ curve to the abscissa to determine the threshold energy.

The curvature of the $I/i$ curve at threshold is determined to an extent by the spread electron energy, but to an even greater extent by the increasing range of energy $R_N$, effective at each point of integration. The departure of the calculated from the measured curve could be modified to the extent of causing the calculated curve to rise to or above the measured one by distorting the measured electron energy distribution to include a broader spread at its base. This does not seem justified at the moment, since theory does not predict the excitation probability except near threshold.

While the results shown in Fig. 5 are not strikingly different from those previously reported by Maier-Leibnitz,[18] Dorrestein,[19] and Schulz,[17] the interpretation of the $i^+$ curve for all of these workers has been obscure due to lack of knowledge concerning the relative contribution to its magnitude of positive ions, the effect of the metastables at the collector surface, and photo electrons produced by radiation, such as that of the $1\,^1S_0-2\,^1P_1$ transition. While the magnitudes of the separated metastable producing mechanisms have never been measured, some indication of the make-up of the $i^+$ curve can follow from observing the excitation efficiency versus energy dependence of other selected transitions, such as the normalized relative intensities previously published by Smit, Heideman, and Smit.[1] Figure 7 indicates the author's version of the threshold excitation of optically measured $S$ and $P$ transitions. All have been measured under the same conditions at $2.5\times10^{-3}$ Torr of helium. Over the wavelength range, the photomultiplier response is relatively constant, so the magnitudes may be compared.

Of the heretofore measured transitions, only those involving $^3S$, $^2S$, and $^3D$ states as initial states show sharply defined intensity peaks within the first volt or so. Triplet and singlet $P$ states exhibit relatively smooth excitation curves peaking at 10 or more volts above threshold. Assuming this information can be transferred to explain the $i^+$ curve of Fig. 5, the two peaks approximately 0.8 V apart must be due to the excitation of the $2\,^3S_1$ and $2\,^1S_0$ levels. Following this reasoning, the onset of $2\,^3S$, the $N=3$ levels (probably $S$ states), and the ionization seem to agree with the assignment of energies shown in Fig. 5. Correcting the intensities of individual series by use of $N^{-3}$ and by omitting the contribution of the higher excitation states, one can use the intensities shown in Fig. 7 to arrive, at least semiquantitatively, at the $N=2$ intensities shown in Fig. 5.

## SUMMARY

Although these results are presented in terms of signal per unit current, and as such are not to be confused with cross sections, they appear to be in general agreement with the theory of Massey and Moisewitsch,[10] except for those results relative to the production of $2\,^1S_0$.

Two resonances in the elastic-scattering cross section have been observed at $19.5\pm0.1$ and $20.3\pm0.1$ V. The first is in reasonable agreement with Schulz, and the second adds to the information concerning elastic resonances predicted by Burke and Schey.[13]

An energy half-breadth for an electron gun has been measured using the elastic-scattering cross section in helium. Its magnitude is of the order of 0.25 V, in contradiction to the greater than 0.5 V measured by Faraday cup retarding measurements.

An example has been presented showing the difference between cross section and the experimentalist's presentation of excitation efficiency or intensity per unit current. Also demonstrated is the relationship of threshold to the excitation-efficiency curve.

## ACKNOWLEDGMENTS

Acknowledgments are due the administrative staff at the Lawrence Radiation Laboratory for support of this work, and to the other members of the Atomic Physics Group for their many contributions.